

An analysis on the impact of large-scale transports of dust pollution on air quality in East Asia as observed in central Korea in 2014

Hak-Sung Kim · Yong-Seung Chung · Ma-Byong Yoon

Received: 4 November 2014 / Accepted: 30 December 2014 / Published online: 15 January 2015
© Springer Science+Business Media Dordrecht 2015

Abstract The large-scale transport of dust air pollution in the East Asian region has been being monitored using satellites and ground-based measurements in central Korea for the last 20 years. Severe haze in eastern China as well as dust storms in Mongolia and northern China occurred and moved toward central Korea during the first 5 months of 2014. In addition, severe prolonged haze in eastern China occurred on a large scale in February 2014. The daily mass concentrations originating from haze and dust storms at a background observation site in central Korea exceeded the air quality standard of PM10 ($100 \mu\text{g m}^{-3} \text{ day}^{-1}$) and PM2.5 ($50 \mu\text{g m}^{-3} \text{ day}^{-1}$). Dust loadings caused by dust air pollution from Mongolia and China are clearly worsening the air quality in the background area in central Korea. Anthropogenic dust pollution from severe haze loads dust particulates finer than $2.5 \mu\text{m}$. On the other hand, a natural dustfall case originating from a dust storm usually loads coarse dust particulates in the atmosphere. The impact of dust storms on air quality varies depending on the passing route in East Asia.

Keywords Haze · Dust storm · Dust air pollution · Anthropogenic dust pollution case · Natural dustfall case · Impact of dust air pollution

H.-S. Kim (✉) · Y.-S. Chung
Korea Centre for Atmospheric Environment Research, 304
Koonghyon, Khangnae, Cheongju, Chungbuk 361-891, Korea
e-mail: enviro07@chol.com

M.-B. Yoon
Department of Science Education, Jeonju University, 303 Cheonjam,
Wansan, Jeonju, Cheonbuk 560-759, Korea

Introduction

Emissions of air pollutants are on a steady rise with economic and industrial development in the East Asian region (Streets and Waldhoff 2000; Seinfeld et al. 2004). The rapid development of China is responsible for the consumption of 2.91 billion tons of fossil fuel (Korea Energy Economics Inst. 2012). In 2005, the combustion of fossil fuels emitted 2774, 1824, and 994 kt of TSP, PM10, and PM2.5, respectively (Zhao et al. 2008). It resulted in extremely severe and persistent haze occurrences in eastern and central China in January 2013 which was reported as the haziest month in the past 60 years in Beijing (Lu et al. 2013). In addition, eastern China was shrouded in prolonged fog and haze during February 2014. On the other hand, dust storms generally occur in northern China and Mongolia in the spring and are transported to Korea, Japan, and as far as the USA (McKendry et al. 2001; Kurosaki and Mikami 2003; Wang and Fang 2006).

Many modelling approaches and techniques have been used to forecast dust air pollution, including dust storm and anthropogenic dust pollution (Carnevale et al. 2012; Tan et al. 2012; Wang and Niu 2013; Sun et al. 2013a, b). At the same time, studies have been conducted on the long-range transport of dust air pollution related to synoptic scales in the East Asian region (Kurosaki and Mikami 2003; Wang and Fang 2006; Kim et al. 2014a). Dust air pollution in East Asia affects air quality in the leeward side in varying ways depending on the origin and the passing route. Air quality standards of dust air pollution in Korea are defined as PM10 ($100 \mu\text{g m}^{-3} \text{ day}^{-1}$) and PM2.5 ($50 \mu\text{g m}^{-3} \text{ day}^{-1}$). Therefore, it is necessary to conduct a quantitative evaluation of the impact of dust pollution cases on air quality.

Operational monitoring makes it possible to observe the different origins of air pollution, distinguish aerosol types, and compare satellite data with surface mass concentrations

(Chung and Kim 2008; Kim and Chung 2008; Logan et al. 2013). The variations of TSP, PM₁₀, and PM_{2.5} and the causes were analyzed through long-term observations (Kim et al. 2014b). The purpose of this observational study is to analyze the impact of dust air pollution on the air quality of some of the typical dust pollution cases which occurred in central Korea during the first 5 months of 2014.

Measurements and analyses

Operational monitoring has been conducted since 1993 at the Korea Centre for Atmospheric Environment Research (KCAER) in Cheongju, a rural location in central South Korea (Fig. 1). The geographical environment and instruments of KCAER were introduced in previous studies (Kim and Chung 2008; Kim et al. 2014a). The observatory is located approximately 120 km south of Seoul and 120 km east downwind of the Tae-ahn Peninsula on the west coast of the Korean Peninsula. In the case of moderate winds, it takes roughly 3–5 h for the airflow from Tae-ahn to reach the observatory. There are no large cities or industrial complexes between the Tae-ahn Peninsula and the observatory.

The mass concentrations of TSP, PM₁₀, and PM_{2.5} particulate matters were measured by using the TEOM Series 1400a by Rupprecht & Patashnick, which is designed to measure the mass of dust collected in a filter by means of the tapered element oscillating microbalance (TEOM) method. The RGB-composite images of National Oceanic and Atmospheric Administration (NOAA) satellites are created using three channels, including 1, 2, and 4, from the Advanced Very High Resolution Radiometer (AVHRR) data. It is possible to distinguish the particles according to the sensitivity of visible rays and near-infrared rays from dust storms and anthropogenic dust pollution in the atmosphere, and by the difference in the absorption of thermal infrared rays (Chung and Le 1984; Chung and Kim 2008). RGB-composite images display

the seas and lakes in blue, typically without air pollution due to its low reflection rate. The clouds appear in white and the land in green. Anthropogenic dust pollution images of the seas and lakes appear in magenta, and dust storms appear in purplish yellow. With NOAA satellites, of which 18 and 19 are now operational, the occurrence and transport of large-scale air pollution can be observed by directly receiving AVHRR data twice a day.

Results and discussions

Mass concentration measurements at the rural site in central Korea

The long-range transport of severe haze and dust storms during winter and spring is classified based on measurements of mass concentrations of different particle sizes and satellite observation. Figure 2 shows the day-to-day variation of daily maximum mass concentrations measured at KCAER between January and May 2014. The average values of daily TSP, PM₁₀, and PM_{2.5} were 68 ± 32 , 49 ± 25 , and $29 \pm 17 \mu\text{g m}^{-3}$, respectively. Mass concentrations of PM₁₀ measured in downtown Cheongju, which is east of the observation site, reached $88 \pm 58 \mu\text{g m}^{-3}$. Between January and May 2014, there were five anthropogenic dust pollution cases (8 days) and three natural dustfall cases (5 days). Also, TSP mass concentration increased sharply to $344 \mu\text{g m}^{-3}$ on May 2, 2014, where pine pollen dispersed into the atmosphere in that area.

Anthropogenic dust pollution cases from severe haze in eastern China

Eastern China was covered with severe prolonged haze from February 21 to 26, 2014, and then the haze moved to the Korean Peninsula on a synoptic scale (Fig. 3). The total areas

Fig. 1 Map of the East Asian region and annual PM_{2.5} exposure from 2008 to 2010 (van Donkelaar et al. 2010). Tae-ahn (T) and Korea Centre for Atmospheric Environment Research (KCAER) are the background monitoring stations in central Korea

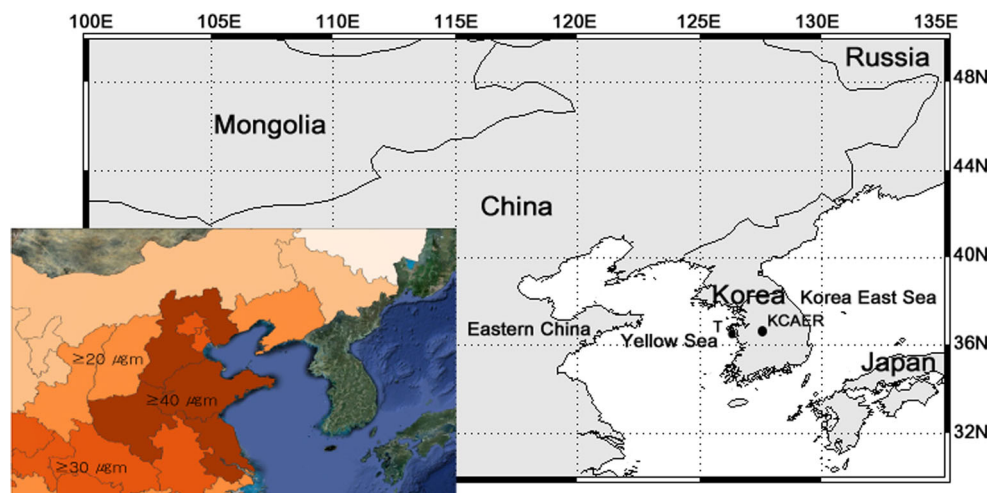
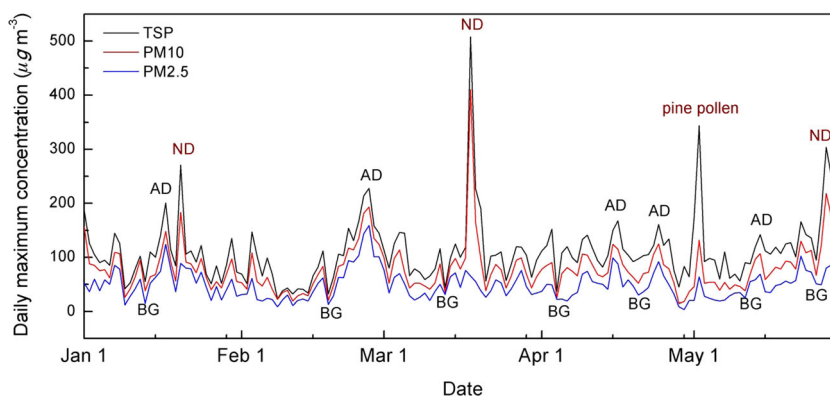


Fig. 2 Variations of daily maximum TSP, PM10, and PM2.5 measured at KCAER from January to May in 2014 (*AD* refers to an anthropogenic dust pollution case, *ND* refers to a natural dustfall case, and *BG* refers to a background airflow case)



under haze reached 2.07 million km² at the height of its dispersion, covering 11 provinces in northern China (NCC 2014). On February 21 (Fig. 3a), severe haze developed on a large scale in eastern China, located at the rear of a high-pressure system over the Yellow Sea. A NOAA satellite RGB-composite image (1619 LST, February 21) also shows haze occurring in the eastern part of China on a large scale and air pollution originating from north of the Shandong Peninsula expanding eastward with the west-northwesterly airflow. Additionally, the north-northeasterly wind was blowing over toward the Korean Peninsula. The cumulus developed sequentially in the direction of north to south in the southern parts of both the Yellow Sea and Jeju Island. TSP, PM10, and PM2.5 decreased to 43, 31, and 19 µg m⁻³, respectively, at 1300 LST on February 21 (Fig. 4).

On February 22 (Fig. 3b), a high-pressure system over the Yellow Sea slowly expanded toward the Korea East Sea, subjecting the Korean Peninsula to the influence of a stagnant high-pressure system. Cumulus that developed over the Yellow Sea had dissipated in the NOAA satellite RGB-composite image by 1607 LST, February 22. Furthermore, haze was observed in eastern China at the rear of a high-pressure system, and air pollution in the north of the Shandong Peninsula affected the Korean Peninsula due to northwesterly winds. Under the influence of a continuous stagnant high-pressure system on February 23 (Fig. 3c), haze developed in eastern China, and large-scale air pollution was distributed over the Yellow Sea and the Korean Peninsula. The mass concentrations of TSP, PM10, and PM2.5 gradually increased between February 22 and 23 (Fig. 4).

Eastern China, the Yellow Sea, and the Korean Peninsula were located at the rear of a high-pressure system as the other high-pressure system developing in Mongolia expanded southeastward between February 24 and 25 (Fig. 3d). Haze continuously occurred in eastern China, and large-scale air pollution was distributed from the north of the Shandong Peninsula to the Korean Peninsula in the NOAA satellite RGB-composite image (1358 LST, February 25). On February 26 (Fig. 3e), a low-pressure system moved from southern China to the south of Jeju Island. This resulted in precipitation

in the southern part of the Korean Peninsula and caused south-southeasterly airflow into central Korea. The clouds covered as far as central Korea in the NOAA satellite RGB-composite image (1347 LST, February 26). Between February 24 and 26 (Fig. 4), mass concentrations gradually increased and peaked at 1100 LST on February 26. Daily averages of PM10 and PM2.5 exceeded the air quality standard in Korea between February 24 and 26. However, mass concentrations rapidly decreased on the afternoon of February 26 with a south-southeasterly wind.

The observatory was located ahead of, in the centre of, and at the rear of high pressure on February 21, between February 22 and 23, and between 24 and 26, respectively (Fig. 5). In Fig. 4, daily variations of mass concentrations peaked between February 22 and 26 at 1000~1100 LST as a result of the large-scale transport of anthropogenic air pollution from eastern China. As a rule, cities having more air pollutant emissions show a high level of air pollutants at dawn when the mixing layer height stays low. The mixing layer height shows daily variations where the height starts to rise at 0900 LST, peaking at 1500 LST. Mass concentrations peaked on the surface due to a vertical mixture in the morning when air pollution from eastern China flowed into central Korea. However, after mass concentration reached its peak at 1100 LST on February 23, it sharply dropped at 1500 LST when the height of the mixing layer reached its maximum. It can be argued that the continuous transport of air pollution from eastern China located at the rear of the high-pressure system was delayed since KCAER was located in the centre of a high-pressure system on February 23, and the concentrations again increased on February 24.

Natural dustfall cases due to dust storms

The background airflow case was observed with a surface weather chart and an RGB-composite image on March 13 before the occurrence of the dustfall case in central Korea on March 16~18, 2014 (Fig. 6). The chart illustrates that the low-pressure system developing along the Yangtze River in southern China moved northeastward toward Japan on March 13 (Fig. 6a). This caused precipitation of 26.0 and 1.0 mm in

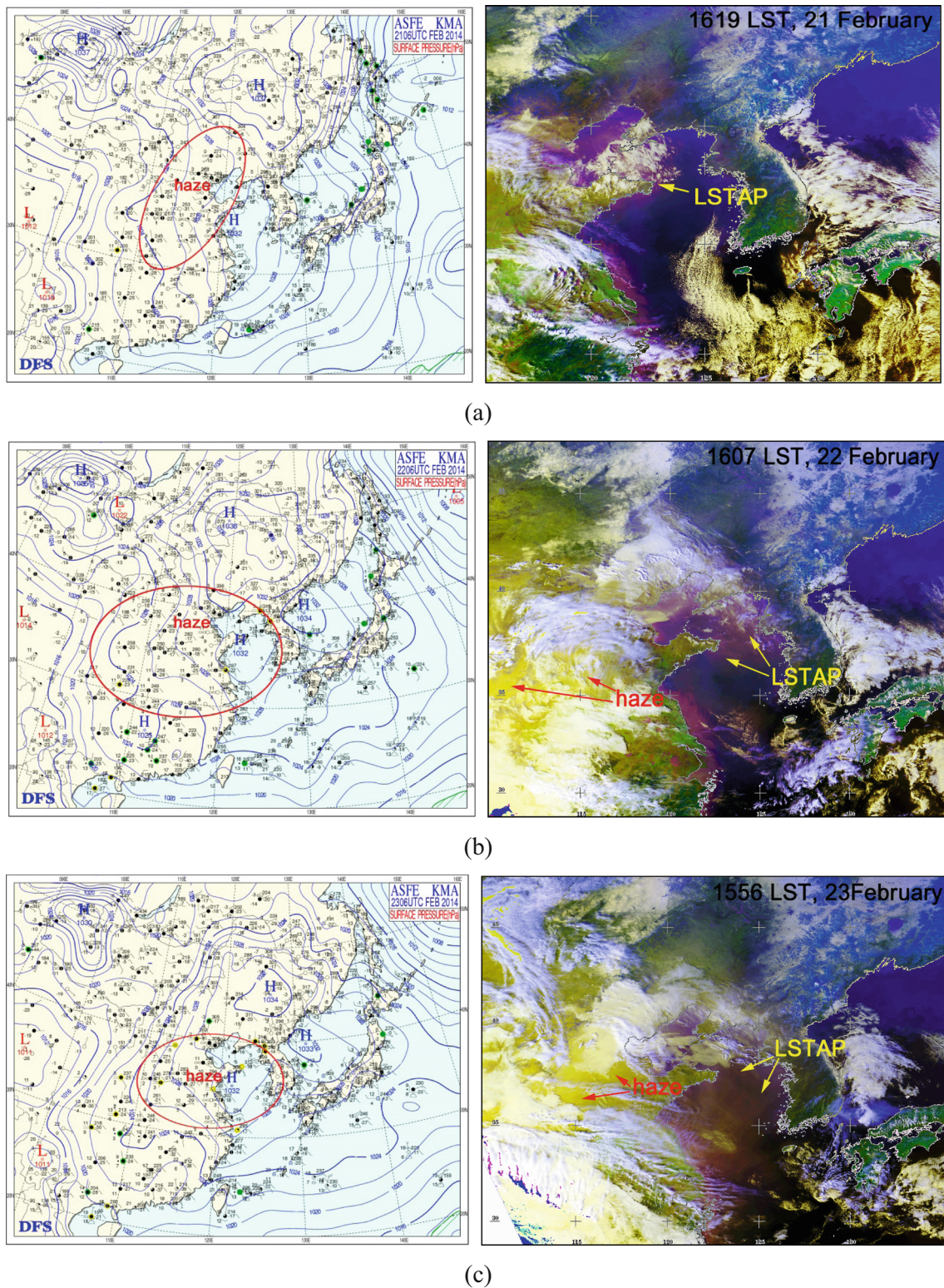


Fig. 3 a–e Surface meteorological charts (*left*) and NOAA satellite RGB-composite images (*right*) showing haze in eastern China and large-scale transport of anthropogenic air pollution (*LSTAP*) over the Yellow Sea from February 21 to 26, 2014

central Korea on March 12 and March 13, respectively. In addition, north-northeasterly winds swept across the Yellow Sea and the Korean Peninsula on the forward side of an

anticyclone expanding over northern China all the way down to southern China. A NOAA satellite RGB-composite image shows that cumulus developed to the south of the Yellow Sea

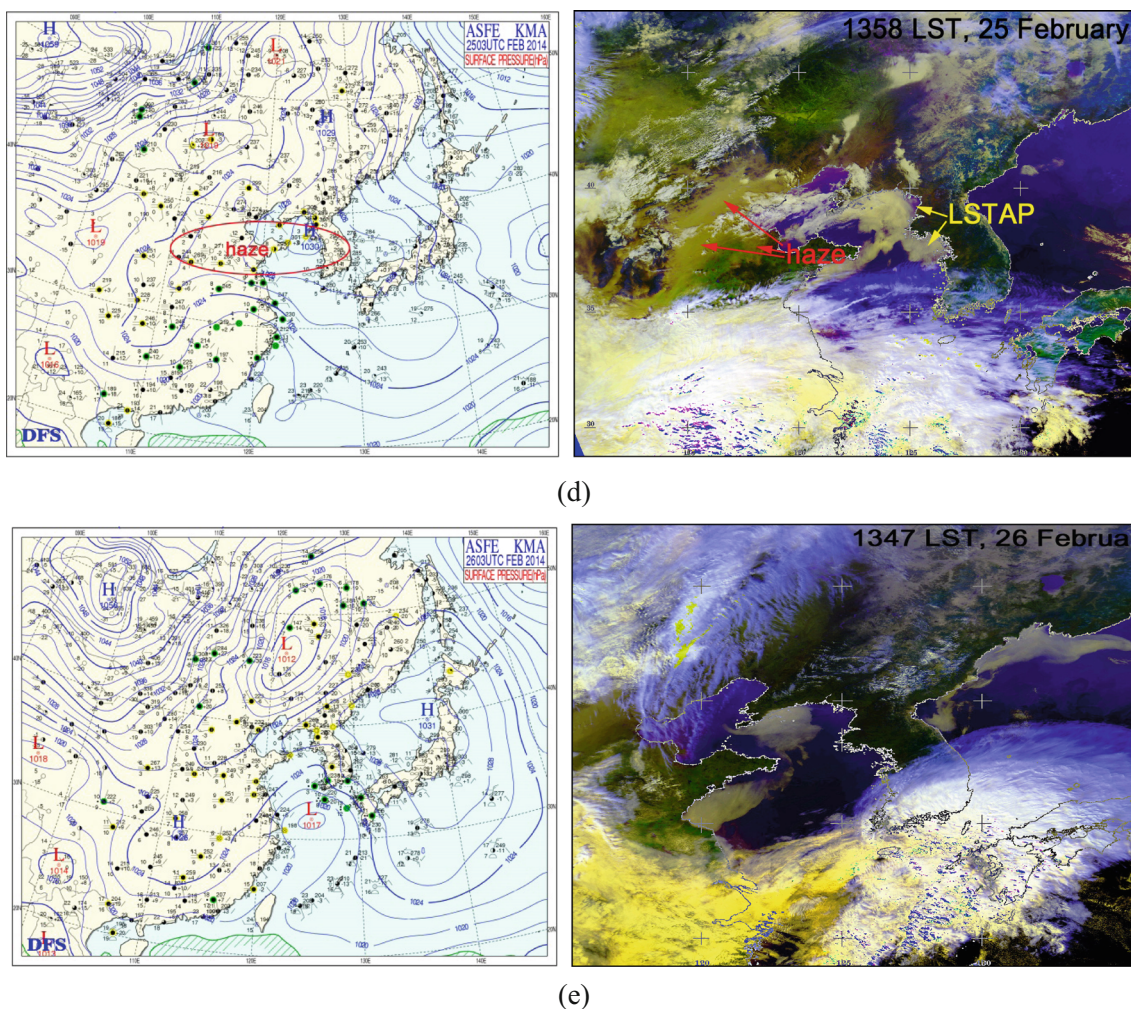


Fig. 3 (continued)

(Fig. 6b). Daily averages of TSP ($27 \mu\text{g m}^{-3}$), PM10 ($22 \mu\text{g m}^{-3}$), and PM2.5 ($16 \mu\text{g m}^{-3}$) were low due to the precipitation and the north-northeasterly airflows on March 13 (Fig. 8).

On the other hand, Fig. 7 illustrates meteorological charts and NOAA satellite RGB-composite images showing dust storm observations for March 16~18, 2014. On March 16 (Fig. 7a), central Mongolia was located on the forward side

Fig. 4 Variations of hourly TSP, PM10, and PM2.5 mass concentrations measured at KCAER between February 20 and 28, 2014. Gray areas are the background airflow case and anthropogenic dustfall case

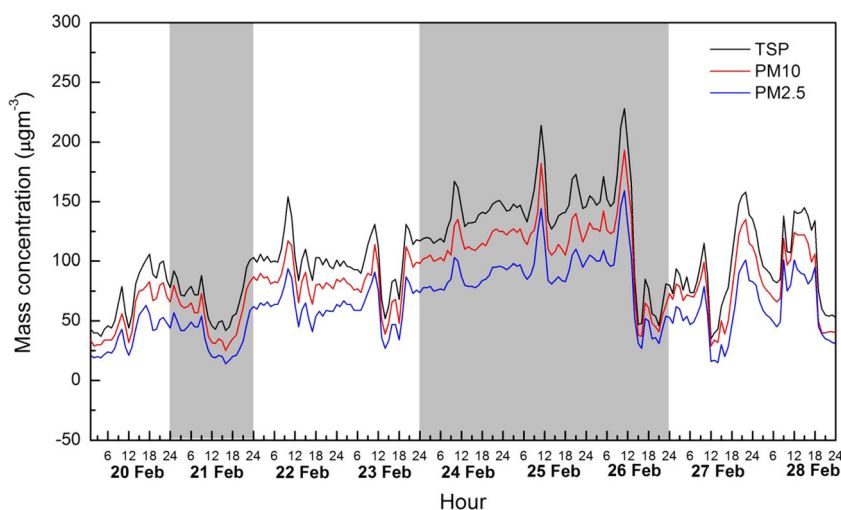
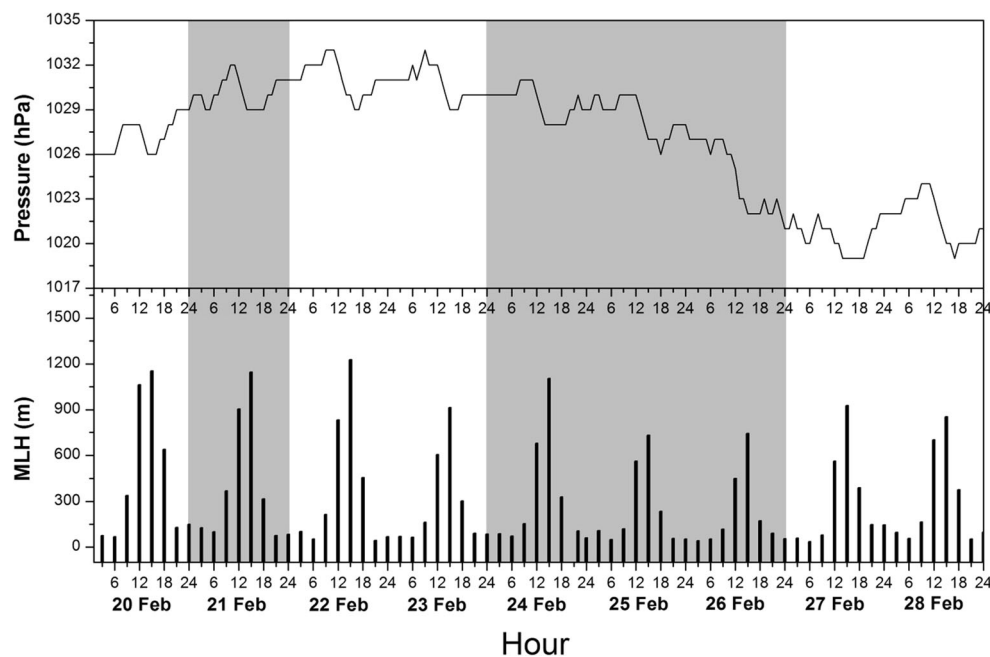


Fig. 5 Variations of hourly pressure and mixing layer height calculated at KCAER between February 20 and 28, 2014. Gray areas are the background airflow case and anthropogenic dustfall case



of an intense anticyclone and at the rear of a low-pressure system. The surface wind was over 10 m s^{-1} due to a strong pressure gradient. The NOAA RGB-composite image shows dust being blown upward into the atmosphere in central Mongolia. On March 17 (Fig. 7b), a dust storm was located at the rear of a cold front of a cyclone that moved toward the north-northwest of the Korean Peninsula and ahead of an expanding anticyclone. On March 18 (Fig. 7c), as the centre of low pressure was moving toward the northeast of the Korean Peninsula, the cold front lying northeast-southwest passed through the Korean Peninsula to the Korean East Sea. Dust storms moved into the central part of the Korean Peninsula ahead of the high-pressure system with the north-northeast airflow.

A natural dustfall case lasted 13 h on March 18, and TSP and PM10 mass concentrations rose to 508 and $410 \mu\text{g m}^{-3}$, respectively (Fig. 8). However, PM2.5 mass concentrations of $65 \mu\text{g m}^{-3}$ did not rise as high as those on other days. The dust loadings on the dusty day show that most of the dust in the atmosphere was distributed with coarse dust particulates larger than $2.5 \mu\text{m}$. Daily averages of TSP and PM10 were 211 and $160 \mu\text{g m}^{-3}$, respectively, on March 18, thus exceeding the air quality standard of PM10 in Korea.

Observations of background mass concentrations

The northern part of the Korean Peninsula has less air pollutant emissions than the eastern part of China (Fig. 1). Accordingly, north-northwesterly airflow resulted in a background airflow case when the Korean Peninsula was located in the forward side of an anticyclone. The background mass concentrations at KCAER refer to those cases when particulate matter

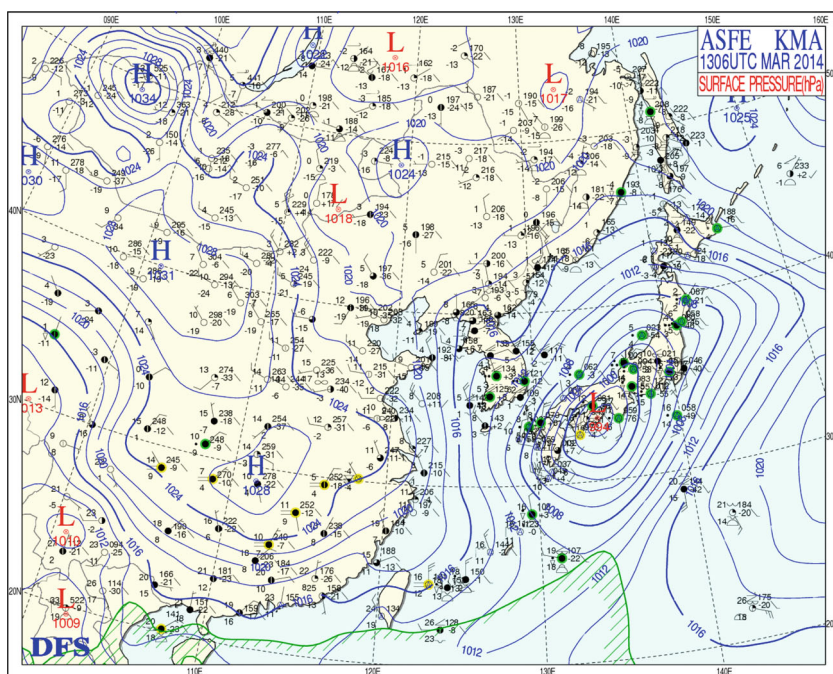
in the atmosphere has been washed out or rained out by precipitation due to a low-pressure center. Background mass concentrations could be a criterion by which to quantitatively estimate low air quality.

Table 1 shows the daily mass concentrations and a synoptic feature in the background airflow cases within 10 days right before an anthropogenic dust pollution case and a natural dustfall case occurred at KCAER. Daily averages of TSP, PM10, and PM2.5 of the background airflow case prior to the anthropogenic dust pollution case registered 49 , 33 , and $19 \mu\text{g m}^{-3}$, respectively, and the daily averages of TSP, PM10, and PM2.5 prior to the natural dustfall case reached 41 , 30 , and $18 \mu\text{g m}^{-3}$, respectively.

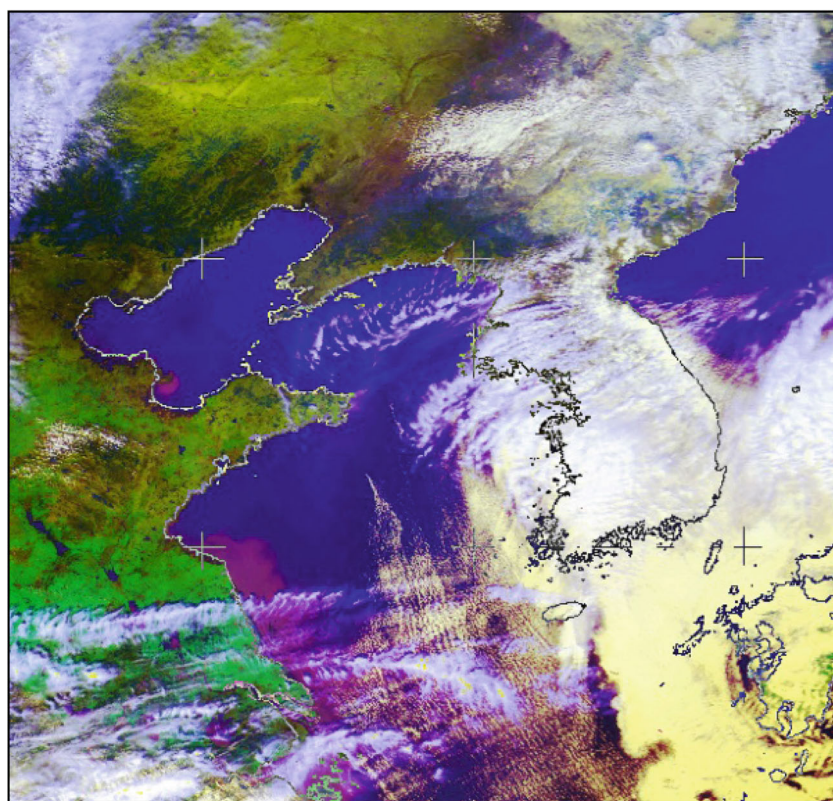
Impact of dust air pollution case on air quality

Table 2 shows daily averages of TSP, PM10, and PM2.5 in an anthropogenic dust pollution case and a natural dustfall case between January and May 2014. The average mass concentrations of TSP, PM10, and PM2.5 reached 120 , 93 , and $70 \mu\text{g m}^{-3}$, respectively, in the anthropogenic dust pollution case. However, average mass concentrations of TSP, PM10, and PM2.5 in dustfall cases registered 162 , 118 , and $52 \mu\text{g m}^{-3}$, respectively. In case 6, the maximum hourly values reached as high as 271 , 183 , and $89 \mu\text{g m}^{-3}$ though daily averages of TSP, PM10, and PM2.5 were low. The case 7 shows higher TSP and PM10 mass concentration levels compared with cases 6 and 8, and the PM2.5 mass concentration levels turned out lower. Accordingly, the PM2.5/TSP daily mass concentration ratio reached 20% , a level lower than in cases 6 and 8 rated at 45 and 35% , respectively. The dust storm of case 7 was transported into the Korean Peninsula with north-northwest

Fig. 6 **a** A surface meteorological chart (1500 LST) and **b** a NOAA satellite RGB-composite image (1425 LST) showing the north-northeasterly airflow over the Yellow Sea region and rainfall in central Korea on March 13, 2014



(a)



(b)

airflow; thus, this dust storm did not pass through eastern China. While TSP and PM10 mass concentrations in the anthropogenic dust pollution case originating from eastern China were lower than those in the natural dustfall case, the PM2.5

mass concentration was higher in the anthropogenic dust pollution case. The average PM2.5/TSP mass concentration ratio in the anthropogenic dust pollution case reached 58 %, a level higher than 32 % of the natural dustfall case.

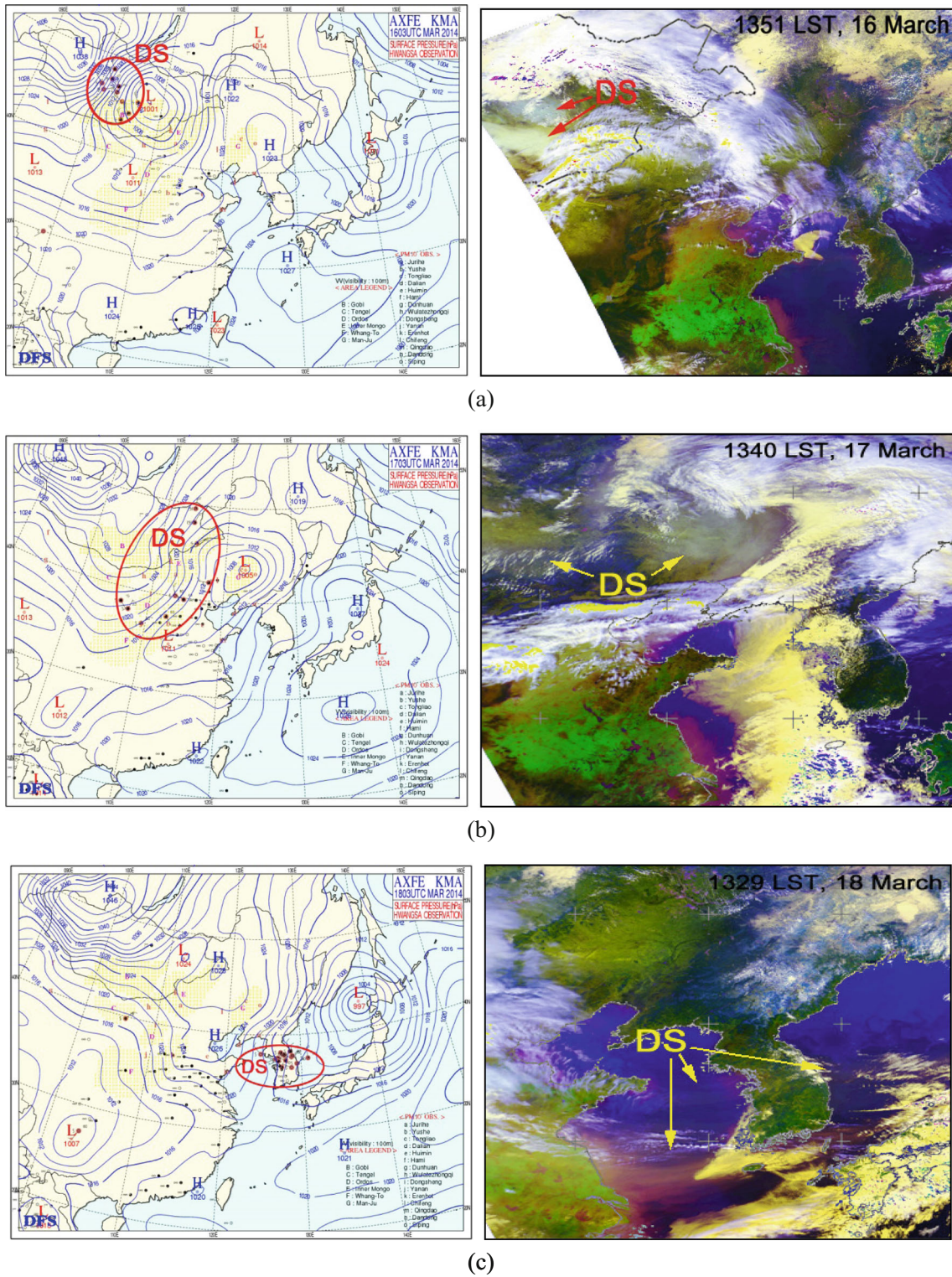
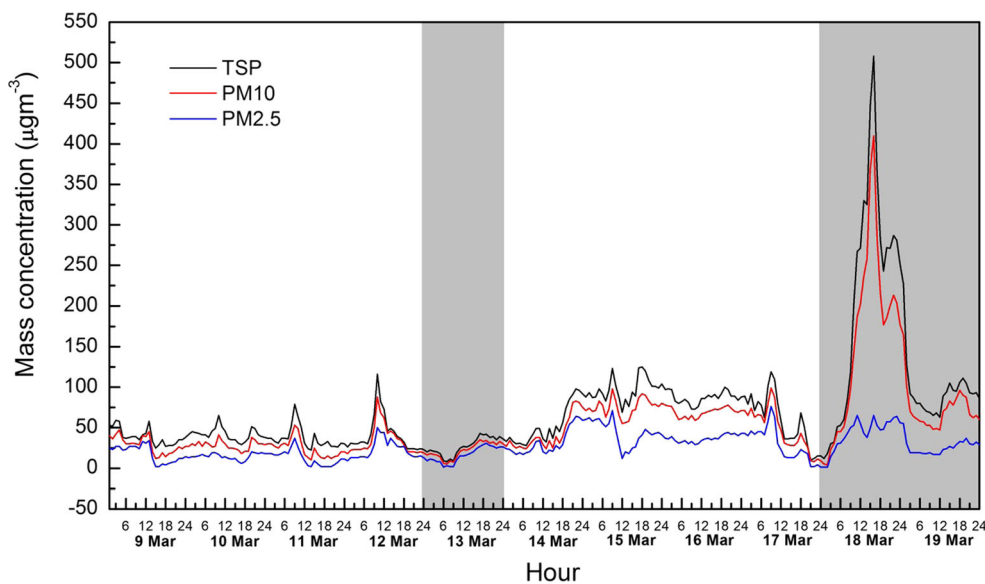


Fig. 7 a–c Surface meteorological charts (*left*) and NOAA satellite RGB-composite images (*right*) showing the occurrence and transport of dust storms (DS) over the East Asian region between March 16 and 18, 2014

Table 3 compares the anthropogenic dust pollution case and the natural dustfall case with regard to the air quality standard of PM10 and PM2.5 in Korea between January and May 2014. The observed daily PM10 concentrations of

8 days exceed the upper limit value defined in the air quality standard of PM10. The number of days exceeding PM10 concentration standards in anthropogenic dust pollution cases and natural dustfall cases is 4 days each.

Fig. 8 Variations of hourly TSP, PM10, and PM2.5 mass concentrations measured at KCAER between March 9 and 19, 2014. Gray areas are the background airflow case and natural dustfall case



Furthermore, of the 18 days where the air quality standard of PM2.5 was exceeded, anthropogenic atmospheric pollution cases were observed on 12 days, and natural dustfall cases on 3 days. Air quality in central Korea is

Table 1 Daily average mass concentrations of TSP, PM10, and PM2.5 and major synoptic and weather conditions on the day of background airflow before the anthropogenic dust pollution case and the natural dustfall case occurred from January to May in 2014

Case	Case number	Date	TSP ($\mu\text{g m}^{-3}$)	PM10 ($\mu\text{g m}^{-3}$)	PM2.5 ($\mu\text{g m}^{-3}$)	PM2.5/TSP (%)	Main synoptic and weather conditions
Background airflow case before an anthropogenic dust pollution case	1	13 January	36	26	7	19	The Korean Peninsula experienced persistent strong north-northwesterly winds due to a high-pressure system over the Chinese mainland.
	2	21 February	69	54	36	52	A cyclone located northeast of the Korean Peninsula and a high-pressure system stagnant over the Chinese mainland caused north-northeasterly winds.
	3	4 April	23	13	7	30	A cold front passed the Korean Peninsula on April 3; north-northwesterly winds blew on April 4 due to a stagnant high-pressure system over the Chinese mainland
	4	21 April	68	46	26	38	A moving anticyclone was stagnant over the southern part of China. The Korean Peninsula was ahead of a moving anticyclone.
	5	11 May	50	27	18	36	A cyclone passed the Korean Peninsula from China to the East Sea of Korea, causing rainfall (16.0 mm).
		Average	49	33	19	39	
Background airflow case before a natural dustfall case	6	13 January	36	26	7	19	The Korean Peninsula experienced persistent strong north-northwesterly winds due to a high-pressure system over the Chinese mainland.
	7	13 March	27	22	16	59	The Korean Peninsula located at the rear of a cyclone over Japan caused rainfall (1.0 mm) and north-northeasterly wind.
	8	25 May	59	42	31	53	A slow-moving cyclone passed the Korean Peninsula from China to the Korean East Sea; which caused rainfall (3.5 mm).
			Average	41	30	18	44

Table 2 Daily average mass concentrations of TSP, PM10, and PM2.5 and major synoptic features for anthropogenic dust pollution cases and natural dustfall cases observed at Cheongju from January to May in 2014

Case	Case number	Date	TSP ($\mu\text{g m}^{-3}$)	PM10 ($\mu\text{g m}^{-3}$)	PM2.5 ($\mu\text{g m}^{-3}$)	PM2.5/TSP (%)	Major synoptic features
Anthropogenic dust pollution case	1	17 January	127	102	77	61	A large anticyclone covered the Chinese mainland and the Yellow Sea region.
	2	24 February	135	113	85	63	A large anticyclone covered a wide area ranging from eastern China to Japan.
		25 February	151	125	97	64	
		26 February	122	101	81	66	
	3	15 April	100	71	53	53	A slow-moving anticyclone was stagnant over the Yellow Sea region.
16 April		117	77	58	50		
4	24 April	109	79	60	55	A slow-moving anticyclone was stagnant over the Yellow Sea region.	
5	14 May	96	74	47	49	A cyclone was located to the northeast of the Korean Peninsula. The Korean Peninsula experienced persistent west-northwesterly airflow from eastern China.	
		Average	120	93	70	58	
Natural dustfall case	6	20 January	80	60	36	45	A cyclone moved slowly from Mongolia to the Korean Peninsula and passed through eastern China. A dust storm between the rear of a cold front and ahead of an anticyclone passed through eastern China.
	7	18 March	211	160	43	20	A cyclone passed the northern part of the Korean Peninsula from Mongolia. A dust storm with a northeasterly airflow lasted until March 18 ahead of a large anticyclone.
	8	27 May	181	131	55	30	A cyclone moved slowly from Mongolia to the Korean Peninsula, passing through eastern China. A dust storm at the rear of a cold front passed through eastern China.
		28 May	195	136	65	33	
		29 May	142	104	61	43	
		Average	162	118	52	32	

affected by long-range large-scale transport of air pollution from China.

Conclusions

After an extremely severe haze persisted in eastern and central China in January 2013, another severe haze occurred and continued on a large scale over eastern China during February

2014. Air pollution transported on a wide scale in East Asia was observed through satellites and air quality measurements taken at a background observation site in central Korea. This study observed the occurrence and transport of five anthropogenic dust pollution cases and three natural dustfall cases between January and May 2014, and analyzed the impact of those cases on air quality.

Background airflow cases can be observed in consideration of the distribution of air pollutants and the transport of airflow of synoptic scales. Background airflow cases were observed

Table 3 Number of days when daily mass concentrations exceeded the air quality standards of PM10 and PM2.5 in Korea with the large-scale transport of anthropogenic air pollution and dust storms from January to May 2014

Type	PM10 (days)	PM2.5 (days)
Air quality standard of mass concentration ($\mu\text{g m}^{-3} \text{ day}^{-1}$)	100	50
Mass concentration criteria of a natural dustfall case used by KCAER ($\mu\text{g m}^{-3} \text{ h}^{-1}$)	190	85
Number of days when daily mass concentration standards were exceeded	8	18
Number of days when mass concentration standards in Korea were exceeded in anthropogenic dust pollution cases	4	12
Number of days when mass concentration standards in Korea were exceeded in natural dustfall cases	4	3

when the Korean Peninsula was located ahead of an anticyclone and in the presence of a northwesterly airflow, and in the presence of precipitation due to low pressure. The mass concentration in the background airflow cases can be referred to in order to compare dust air pollution cases between January and May 2014.

During this period, the numbers of episode days exceeding the air quality standards of PM10 and PM2.5 were 8 and 18 days, respectively. These episodes were all affected by dust pollution cases. Anthropogenic air pollution occurred when eastern China and the Yellow Sea were located at the rear of a stagnant anticyclone and a migrating anticyclone. This anthropogenic air pollution moved to the Korean Peninsula on a large scale. An anthropogenic dust pollution case with a daily average of PM2.5 concentrations at $70 \mu\text{g m}^{-3}$ ran higher than that of PM2.5 in a natural dustfall case. In an anthropogenic dust pollution case, the air quality standard of PM10 was exceeded on 3 days, and the air quality standard of PM2.5 was exceeded on 12 days. Anthropogenic dust pollution cases generally loaded PM2.5 fine dust in large quantities in the atmosphere in central Korea.

On the other hand, natural dust cases that occurred ahead of an anticyclone developed in Mongolia and northern China and moved toward the Korean Peninsula. In natural dust cases, daily averages of TSP, PM10, and PM2.5 registered 162, 118, and $52 \mu\text{g m}^{-3}$, respectively, and all exceeded the air quality standards in Korea. In natural dust cases in particular, the number of days was 4 when the PM10 air quality standard was exceeded, while the number of days was 4 when the PM2.5 air quality standard was exceeded. While dust loading varied depending on the strength of dustfall occurrences, the case of January 20 that passed the industrial region in eastern China the PM2.5/TSP mass concentration ratio ran higher than the cases of March 18 and May 27–20.

Acknowledgments This study was carried out with a science subvention of the Korea Meteorological Administration, CATER (2012-6160).

References

- Carnevale C, Finzi G, Pisoni E, Volta M, Kishcha P, Alpert P (2012) Integrating Saharan dust forecasts into a regional chemical transport model: a case study over northern Italy. *Sci Total Environ* 418:224–231
- Chung YS, Kim HS (2008) Observations of massive air-pollution transport and associated air quality in the Yellow Sea region. *Air Qual Atmos Health* 1:69–79
- Chung YS, Le HV (1984) Detection of forest-fire smoke plumes by satellite image. *Atmos Environ* 18:2143–2151
- Kim HS, Chung YS (2008) Satellite and ground observations for large-scale air pollution transport in the Yellow Sea region. *J Atmos Chem* 60:103–116
- Kim HS, Chung YS, Choi HJ (2014a) On air pollutant variations in the cases of long-range transport of dust particles observed in central Korea in the leeside of China in 2010. *Air Qual Atmos Health* 7: 309–323
- Kim HS, Chung YS, Kim JT (2014b) Spatio-temporal variations of optical properties of aerosols in East Asia measured by MODIS and relation to the ground-based mass concentrations observed in central Korea during 2001–2010. *Asia Pac J Atmos Sci* 50:191–200
- Korea Energy Economics Institute (2012) Yearbook of energy statistics 31:339pp
- Kurosaki Y, Mikami M (2003) Recent frequent dust events and their relation to surface wind in East Asia. *Geophys Res Lett* 30. doi:10.1029/2003GL017261
- Logan T, Xi B, Dong X, Li Z, Cribb M (2013) Classification and investigation of Asian aerosol absorptive properties. *Atmos Chem Phys* 13:2253–2265
- Lu XY, Tang J, Zhang J, Yue J, Song GK, Hu JG (2013) Annual report on analysis of Beijing society-building. Social Science Academic Press, Beijing
- McKendry IG, Hacker JP, Stull R (2001) Long-range transport of Asian dust to the Lower Fraser Valley, British Columbia, Canada. *J Geophys Res* 106:18361–18370
- National Climate Centre, CMA (2014) Extreme weather and climate events and their impacts in China for the winter December 2012–February 2014. Weather roundup-China
- Seinfeld JH, Carmichael GR, Arimoto R, Conant WC, Brechtel FJ, Bates TS, Cahill TA, Clarke AD, Doherty SJ, Flatau PJ, Huebert BJ, Kim J, Markowicz KM, Quinn PK, Russell LM, Russell PB, Shimizu A, Shinozuka Y, Song CH, Tang Y, Uno I, Vogelmann AM, Weber RJ, Woo JH, Zhang XY (2004) ACE-ASIA: regional climatic and atmospheric chemical effects of Asian dust and pollution. *Bull Am Meteorol Soc* 85:367–380
- Streets DG, Waldhoff ST (2000) Present and future emissions of air pollutants in China: SO₂, NO_x, and CO. *Atmo Environ* 34:363–374
- Sun WY, Yang KJS, Lin NH (2013a) Numerical simulations of Asian dust-aerosols and regional impact on weather and climate—part I: control case-PRCM simulation without dust-aerosols. *Aerosol Air Qual Res* 13:1630–1640
- Sun WY, Yang KJS, Lin NH (2013b) Numerical simulations of Asian dust-aerosols and regional impact on weather and climate—part II: PRCM-dust model simulation. *Aerosol Air Qual Res* 13:1641–1654
- Tan SC, Shi GY, Wang H (2012) Long-range transport of spring dust storms in Inner Mongolia and impact on the China seas. *Atmos Environ* 46:299–308
- van Donkelaar A, Martin RV, Brauer M, Kahn R, Levy R, Verduzco C, Villeneuve PJ (2010) Global estimates of ambient fine particulate matter concentrations from satellite-based aerosol optical depth: development and application. *Environ Health Perspect* 118:847–855
- Wang W, Fang ZY (2006) Numerical simulation and synoptic analysis of dust emission and transport in East Asia. *Glob Planet Change* 52: 57–70
- Wang H, Niu T (2013) Sensitivity studies of aerosol data assimilation and direct radiative feedbacks in modeling dust aerosols. *Atmos Environ* 64:208–218
- Zhao Y, Wang S, Duan L, Lei Y, Cao P, Hao J (2008) Primary air pollutants emissions of coal-fired power plants in China: current status and future prediction. *Atmos Environ* 42:8442–8452